First-Principles Theory of Competing Order Types, Phase Separation, and Phonon Spectra in Thermoelectric $AgPb_mSbTe_{m+2}$ Alloys

S. V. Barabash,[1] V. Ozolins,[1] and C. Wolverton[2]

[1]*Department of Materials Science and Engineering, University of California, Los Angeles, California 90095-1595, USA*
[2]*Department of Materials Science & Engineering, Northwestern University, Evanston, Illinois 60208, USA*

(Received 27 February 2008; revised manuscript received 30 July 2008; published 10 October 2008)

Using a first-principles cluster expansion, we shed light on the solid-state phase diagram and structure of the recently discovered high-performance Pb-Ag-Sb-Te thermoelectrics. The calculated bulk thermodynamics favors the formation of coherent precipitates of ordered $Ag_mSb_nTe_{m+n}$ phases immiscible with rocksalt PbTe, such as $AgSbTe_2$. The solubility is high for Pb in $AgSbTe_2$ and low for (Ag,Sb) in PbTe (8% vs 0.6% at 850 K). The differences in the phonon spectra of PbTe and $AgSbTe_2$ suggest that these precipitates enhance the thermoelectric performance by lowering thermal conductivity.

DOI: 10.1103/PhysRevLett.101.155704 PACS numbers: 64.75.Qr, 61.66.Fn, 63.20.dk, 64.70.kg

Recent measurements [1] of an exceptionally high thermoelectric figure of merit Z ($ZT \sim 2$ at $T = 800$ K) in lead-antimony-silver-telluride (LAST) alloys (conventionally denoted as $AgPb_mSbTe_{2+m}$) demonstrated that these materials are promising candidates for use in thermoelectric power generation devices. The mechanism of the increase in ZT beyond the values achieved in the pure constituents ($ZT \sim 0.8$ in PbTe [2] and $ZT < 1.4$ $AgSbTe_2$ [3]) is not yet clear; it has been suggested [1] to originate from strong compositional fluctuations across the specimens, which could lead to an additional phonon scattering, and thereby to the observed suppression [3,4] of thermal conductivity. The presence of inhomogeneities in high-Z LAST alloys has been demonstrated in several recent studies [1,5–7]. However, currently there is no consensus on the atomic structure of LAST materials, much less on the physical driving force for the formation of the observed inhomogeneities and their relevance to phonon scattering.

In fact, even the structure of the pure ternary $AgSbTe_2$ compound is not reliably established: long thought to have a cubic rocksalt structure with *random* occupation of the cation sublattice [8], $AgSbTe_2$ was recently demonstrated to exhibit *ordering* of Ag and Sb ions [6], but the type of ordering remains elusive [9]. The structure of quaternary alloys between $AgSbTe_2$ and PbTe is even less understood. Most early studies reported that miscible disordered solid solutions exist in the entire concentration range [10–12], although a miscibility gap was also reported [13]. Recent experiments have uncovered strong evidence that many alloys that appear homogeneous in powder x-ray and optical microscopy studies are in fact composed of nano- to micron-scale regions with *varying* composition [7], atomic ordering [6], thermoelectric properties [5], and lattice parameter [6].

On the theoretical side, the largest breakthrough has been the prediction [14] of the likely ordered structures of $AgSbTe_2$. However, only four preselected ordered $AgSbTe_2$ structures were considered [14], leaving open the possibility that the true ground state might have been missed. Moreover, it was not established whether the atomic order survives at the typical processing temperatures (>1000 K). In other studies, ordering tendencies in Pb-containing LAST alloys have only been analyzed using an *ad hoc* model Hamiltonian [15], or assuming that Ag and Sb are present as dilute impurities in PbTe [16,17]. First-principles studies at higher Ag and Sb concentrations have not been attempted, and the composition-temperature phase diagram and phase stability of LAST alloys remains poorly understood.

Here, we report an exhaustive first-principles study of the atomic structure and thermodynamics of ordering and phase-separation in the quasiternary $Pb_{1-x-y}Ag_xSb_yTe$ coherent, rocksalt-based system (i.e., assuming 1:1 cation to anion ratio). We use the cluster expansion method to identify the $T = 0$ K stable ternary ordered arrangements of Pb, Ag, Sb cations on the rocksalt lattice by explicitly searching through $\sim 10^5$ quaternary structures. The calculated composition-temperature phase diagram for the coherent [18,19] $(PbTe)_{1-2x}(AgSbTe_2)_x$ system confirms the existence of a miscibility gap, suggesting that the observed compositional inhomogeneities in LAST thermoelectrics are due to precipitation of ordered $AgSbTe_2$-rich precipitates from the PbTe-rich solid solution. The $AgSbTe_2$ coherent precipitates are predicted to stay ordered up to the melting point of the material. While PbTe tolerates only a small degree of substitution by Ag and Sb on the Pb sites (up to 0.6% at 850 K), the solid solubility of Pb in the ordered $AgSbTe_2$ phase can be as high as 8% at 850 K, with Pb predominantly occupying sites on the Sb sublattice. The ordering temperature of $AgSbTe_2$ is insensitive to the Pb content. Finally, we demonstrate that there are substantial differences in the low-energy region of the phonon spectra of PbTe and $AgSbTe_2$, which are expected to enhance acoustic phonon scattering at matrix-precipitate interfaces and suppress thermal conductivity.

The multicomponent cluster expansion (CE) approach [20] was used to construct an effective Hamiltonian for quasiternary rocksalt-based $Pb_{1-x-y}Ag_xSb_yTe$ structures,

where Pb, Ag, and Sb atoms occupy the cation sublattice of the rocksalt lattice. We used the ATAT toolkit [21] to obtain the optimal set of pair and many-body effective cluster interactions (ECIs), starting from fully relaxed total energies of 86 ordered input structures. The total energies of these structures were calculated within the density-functional theory (DFT) using the VASP code [22]; the calculation details (including a discussion of phonon calculations [23] and of spin-orbit and generalized-gradient corrections) are presented in the auxiliary material [24]. The prediction accuracy of our CE is 6% of the largest formation energy difference between the input structures [24]. The finite-temperature results were obtained with Metropolis Monte Carlo (MC) simulations [21,24]. We account for the local, but not long-range [25], elastic strain (we further analyze the effects of strain in Refs. [19,24]).

Our approach allows us to predict coherent phases. In Fig. 1(a), we show the CE-predicted $T = 0$ K formation energies of all $\sim 10^5$ rocksalt-based ordered structures with less than 20 atoms per unit cell. By constructing a "convex hull" (black lines) such that no structure lies below the planes connecting the vertices of this object, we can identify the stable $T = 0$ K "coherent ground state" structures. All other rocksalt-based structures may lower their energy by phase separating into some of the "coherent ground state" structures. Figure 1(a) shows that the coherent phase stability within the rocksalt-based AgTe-SbTe alloy system is compound-forming and includes several ordered structures [26] besides $AgSbTe_2$, and that all the *quaternary* compounds in the PbTe-(Ag,Sb)Te system are *unstable* with respect to phase separation into PbTe and one of the (Ag,Sb)Te compounds. From the latter observation, we conclude that the observed inhomogeneities [1,5–7] in (Pb,Ag,Sb)Te alloys are coherent nanoscale precipitates of immiscible (Ag,Sb)Te-rich phases.

In addition to the energetics of coherent phases (i.e., those based on the rocksalt lattice), we also consider the known incoherent (Ag,Sb)Te phases [24], as we illustrate in Fig. 1(b). We see that at low temperatures, all the rocksalt-based (Ag,Sb)Te structures discussed in the previous paragraph are, in fact, unstable with respect to phase separation into incoherent nonrocksalt-based phases. However, the energy differences between coherent rocksalt-based and incoherent nonrocksalt-based phases are very small ($\sim$5 meV/atom) for all compounds except SbTe. Such small energy differences might explain why contradictory experimental assessments have been made [12,27] for the relative stability of $AgSbTe_2$ and the equimolar mixture of Ag_2Te and Sb_2Te_3 (see Ref. [24], Sec. 2d). Irrespective of the relative stability of such *bulk* phases, (Ag,Sb)Te-rich coherent *precipitates* inside the PbTe matrix are likely to be constrained to the rocksalt lattice by the large energetic penalty associated with forming an incoherent interface. Note that in Fig. 1(b), we assume 1:1 cation:anion ratio for the aggregate of (Ag,Sb)Te phases; in precipitates, it may be shifted by a finite concentration of defects in the matrix, possibly favoring the incoherent (nonrocksalt) phases.

Among the ground state structures of Fig. 1, energetically the most prominent is $AgSbTe_2$. We find that the lowest energy $AgSbTe_2$ is cubic $D4$; however, it is separated from another structure, trigonal $L1_1$, by only 1.7 meV/cation. $L1_1$ and $D4$ [visualized in Fig. 1(c)] were among the four structures considered earlier by Hoang *et al.* [14]; here, we explicitly confirm that these nearly degenerate structures have the lowest energy among $\sim 10^5$ possible rocksalt-based $AgSbTe_2$ structures. The near-degeneracy of $L1_1$ and $D4$ has a simple geometric reason: the two structures have identical pair- and three-body correlations for *any* neighbor shell [28] (see Section 2b of auxiliary material [24] for definitions and for a discussion of the ways to distinguish $L1_1$ from $D4$ in CE and in experiment [29]). The coherency strain with a surrounding PbTe matrix does not affect $L1_1$ vs $D4$ energetics [19].

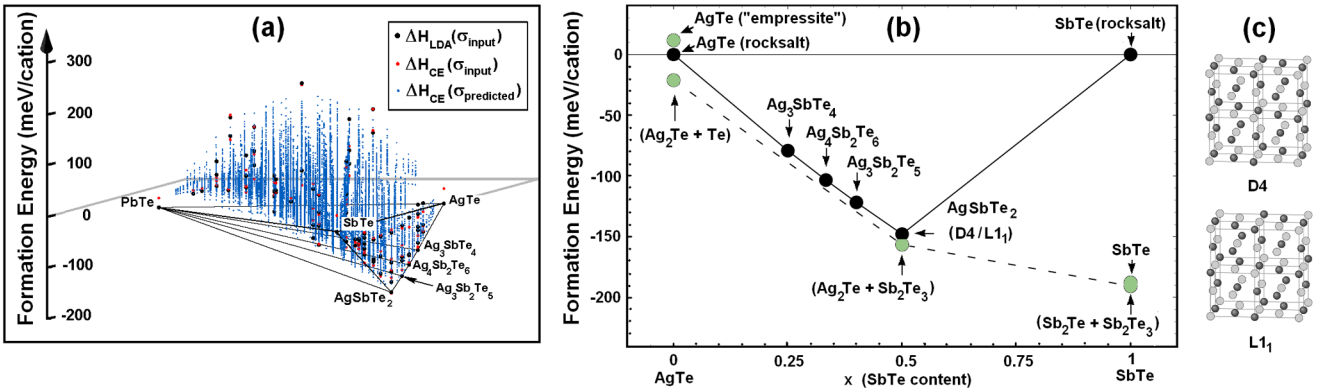

FIG. 1 (color online). (a) The LDA and CE $T = 0$ K formation energies of the 86 "input" (Ag, Pb, Sb)Te structures [large black and gray (red online) points, respectively]. Small gray (blue online) points represent the CE energies of $\sim 10^5$ candidate quaternary structures with $\leq$20 atoms. The black lines highlight the convex hull connecting the "ground state structures" stable within the rocksalt lattice. (b) LDA formation energies of AgTe-SbTe phases at $T = 0$ K. Black dots denote the rocksalt-based structures, gray (green online) dots denote competing nonrocksalt phases and two-phase mixtures. (c) $D4$ and $L1_1$ ordering of Ag and Sb sublattice in $AgSbTe_2$ (for visual clarity, Te sublattice is not shown).

In Fig. 2, we show the isoplethal section of the coherent [18] phase diagram of PbTe-$AgSbTe_2$ solid solutions, as obtained from Monte Carlo simulations [30]. It shows that the ordering tendencies in the $AgSbTe_2$ phase are very strong since the calculated order-disorder transition temperature T_{ord} in the solid state exceeds the experimentally measured melting temperature of pure $AgSbTe_2$. (For a discussion of the hypothetical phase β, see Sec. 3b of Ref. [24].) Furthermore, it is evident that the PbTe phase can accommodate very little substitution by Ag and Sb (only $x_1 \approx 0.6\%$ at the binodal equilibrium at 850 K, or $x_1 \approx 1\%$ at 1000 K); on the contrary, the $AgSbTe_2$ phase accommodates plenty of Pb substitution ($x_2 \approx 8 \pm 4\%$ at 850 K, or more in the presence of coherency strain [19]). The physical reasons for this asymmetry are explored in more depth elsewhere [19], and here we note that in the CE language, the asymmetry is related to the largeness of 3-body ECIs in our CE. Remarkably, despite the large solubility of Pb, the calculated ordering temperature of $AgSbTe_2$ is predicted to remain practically unchanged upon increasing Pb content.

We also indicate in Fig. 2 the experimental melting temperatures T_m of *pure bulk* PbTe and $AgSbTe_2$. An interesting possibility is that in the temperature region between the two bulk melting points, $AgSbTe_2$ precipitates may melt inside a solid PbTe matrix. Similar phenomena have been observed for precipitates in metallic alloys, such as Pb in Al [31]. We hypothesize that heat treatment at temperatures between $T_m(AgSbTe_2)$ and $T_m(PbTe)$ could provide additional means of manipulating the microstructure and ordering of inhomogeneous regions in LAST alloys.

Figure 3(a) shows a Monte Carlo snapshot of the shape of a $AgSbTe_2$ precipitate in PbTe matrix at 800 K. One can observe distinct facets, with the most prominent being (111) facets. Figure 3(b) shows the calculated composition profile across a PbTe/(AgSbPb)Te (111) interface. One can see that the width of this interface is 3–4 cationic layers, suggesting that this interface should be classified as diffuse and entropic contributions to the interfacial free energy are not small. We note here that in our calculations, the precipitate shape is determined only by the interfacial energies and short-ranged atomic relaxation effects; the effects of long-ranged elastic stresses (which tend to "flatten" the precipitates along the elastically soft direction) are not included. The latter are expected to become increasingly important with increasing precipitate size. A parameter characterizing the ratio of the interfacial and elastic energies, $\kappa = l\varepsilon^2 C_{44}/\sigma$ can be used to estimate sizes where elastic effects start to dominate [32]; here, l is the characteristic size of the precipitate, ε is a size misfit between PbTe and (AgSbPb)Te phases, C_{44} is one of the elastic constants, and $\sigma \sim 150$ (mJ/m^2) is our estimated interfacial energy between PbTe and $AgSbTe_2$. The shape of large precipitates ($\kappa > \kappa_{crit} \sim 5.6$) [32] is controlled by the elastic strain. Using the experimental PbTe elastic constant [33] and the calculated lattice mismatch and the interfacial energies, we find that the characteristic size is approximately 15 nm.

Analyzing the atomic structures obtained during MC simulated annealing, we find that $D4$ is clearly thermodynamically preferred over $L1_1$, despite the small energy difference between the two structures [24]. Next, we analyzed the atomic order in the partially ordered structures at $T = 750$ K. We found that at the pure $Ag_{0.5}Sb_{0.5}Te$ composition, both Ag and Sb atoms occupy almost exclusively their respective sublattices. Upon a substitution of 11% of cations by Pb atoms, Ag atoms were found to remain constrained to the Ag sublattice, whereas a substantial fraction of Sb atoms (11%) move to the Ag sublattice [forming Sb antisite defects, see Fig. 3(b)] [30], and most of Pb atoms (92%) fill the Sb sublattice. As we discuss

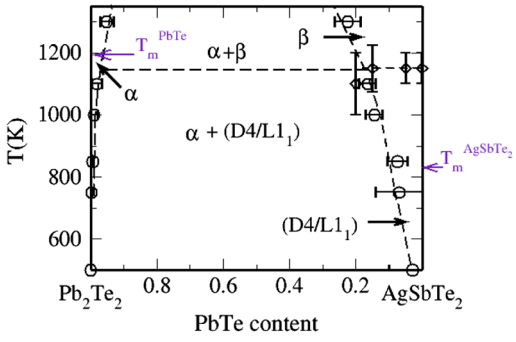

FIG. 2 (color online). Calculated coherent rocksalt-based solid-state phase diagram of $(PbTe)_{1-x}(AgSbTe_2)_{x/2}$, showing the boundaries of the immiscible disordered α and β solid solution phases (circles) and the order-disorder transition temperature T_{ord} for the $(D4/L1_1)$ ordered phase (diamonds). Also marked are the experimental melting temperatures T_m of pure bulk $AgSbTe_2$ and PbTe. All dashed lines are guides for eye.

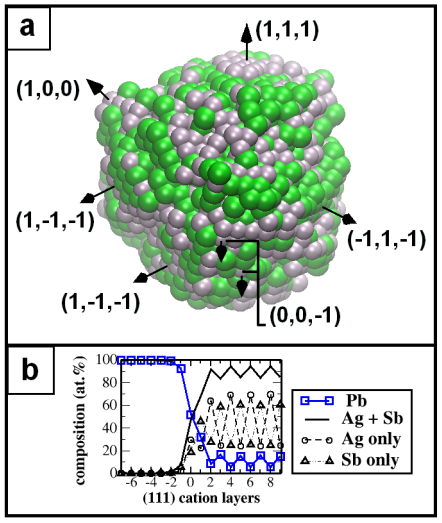

FIG. 3 (color online). (a) Precipitate of a $D4$ $AgSbTe_2$ inside PbTe matrix obtained in Monte-Carlo simulation at 800 K. For clarity, only Ag (light gray) and Sb [dark (green online)] atoms of the precipitate phase are shown. (b) Variation of the atomic composition of (111) cation layers in the vicinity of a (111) boundary between PbTe and $D4$ $AgSbTe_2$.

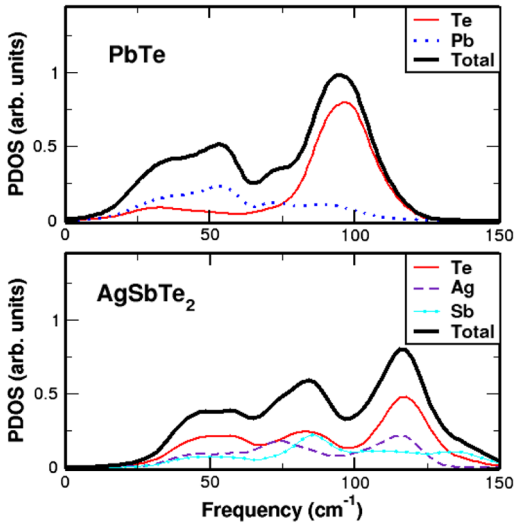

FIG. 4 (color online). Phonon densities of states (PDOS) in rocksalt PbTe and $L1_1$ $AgSbTe_2$ and the partial contributions of constituent ions to the PDOS.

elsewhere [19], this asymmetry has a common energetic origin with the asymmetry of the miscibility gap in Fig. 2. Furthermore, the $Ag_{0.45}Sb_{0.44}Pb_{0.11}Te$ alloy behaves as a hypothetical $Ag_{0.45}X_{0.55}Te$ with *nearly perfect* order possible at that composition. In this sense, Pb atoms do *not* act to suppress the existing ordering, which explains the result that the ordering temperature is practically unchanged by Pb substitution (see Fig. 2).

The calculated phonon densities-of-states (PDOS) for the ideal PbTe and $AgSbTe_2$ phases [24] are shown in Fig. 4. We find that the $AgSbTe_2$ compound is dynamically stable [24] and that its average vibrational frequencies are higher than those of PbTe, consistent with the lighter average atomic mass of the former. The most pronounced differences are seen in the acoustic region, where both the average sound velocity (as measured by the inverse cubic root of the curvature of the PDOS near $\omega = 0$) and the partial mode Te character are smaller in PbTe than in $AgSbTe_2$. Accordingly, in PbTe the Te ions constitute the optical frequency peak centered around 95 cm^{-1}, while the Pb ions dominate in the acoustic region. In $AgSbTe_2$, due to the closer similarity of the ionic masses, the vibrational mode character is roughly evenly distributed between the cations and anions at both acoustic and optical frequencies.

The above structural and PDOS calculations suggest that several effects may combine to cause the significant lowering of thermal conductivity observed in LAST alloys: (i) atomic-scale roughness of the precipitate-matrix interface shown in Fig. 3, (ii) mismatch of the acoustic velocities between the precipitates and the matrix, and (iii) mismatch of the ionic character of the vibrational modes, causing bending and scattering of acoustic waves.

The authors gratefully acknowledge financial support from NSF under Grants No. DMR-0427638 (S. B. and V. O.) and CBET-0730929 (C. W.) and from the FCRP Focus Center for Functional Engineered Nano Architectonics (S. B. and V. O.).

[1] K. F. Hsu *et al.*, Science **303**, 818 (2004).
[2] Z. H. Dughaish, Physica B (Amsterdam) **322**, 205 (2002).
[3] R. F. Rosi *et al.*, Adv. Energy Convers. **1**, 151 (1961); RCA Rev. **22**, 82 (1961).
[4] T. Ono *et al.*, J. Phys. Soc. Jpn. **17**, 1070 (1962).
[5] Nancy Chen *et al.*, Appl. Phys. Lett. **87**, 171903 (2005).
[6] E. Quarez *et al.*, J. Am. Chem. Soc. **127**, 9177 (2005).
[7] H. Lin *et al.*, Phys. Rev. B **72**, 174113 (2005).
[8] S. Geller and J. H. Wenick, Acta Crystallogr. **12**, 46 (1959).
[9] Several types of order in $AgSbTe_2$ suggested in Ref. [6] reasonably match the observed diffraction patterns.
[10] H. Fleischmann, Z. Naturforsch. **16a**, 765 (1961) (in German).
[11] L. Borisova and S. Dimitrova, Phys. Status Solidi A **53**, 403 (1979); L. Borisova, Phys. Status Solidi B **126**, K155 (1984).
[12] R. G. Maier, Z. Metallkd. **54**, 311 (1963) (in German).
[13] H. Rodot, Compte rendu **249**, 1872 (1959) (in French).
[14] K. Hoang *et al.*, Phys. Rev. Lett. **99**, 156403 (2007).
[15] K. Hoang *et al.*, Phys. Rev. B **72**, 064102 (2005).
[16] D. Bile *et al.*, Phys. Rev. Lett. **93**, 146403 (2004).
[17] H. Hazama *et al.*, Phys. Rev. B **73**, 115108 (2006).
[18] Here we define "coherent" alloys as "constrained to the rocksalt-based lattice," reflecting the coherent conditions inside PbTe matrix. For the discussion of the strain effects, see Ref. [19].
[19] S. V. Barabash, V. Ozolins, and C. Wolverton (to be published).
[20] J. M. Sanchez *et al.*, Physica A (Amsterdam) **128**, 334 (1984).
[21] A. van de Walle *et al.*, CALPHAD: Comput. Coupling Phase Diagrams Thermochem. **26**, 539 (2002).
[22] G. Kresse and J. Hafner, Phys. Rev. B **48**, 13115 (1993); G. Kresse and J. Furthmuller, Comput. Mater. Sci. **6**, 15 (1996); Phys. Rev. B **54**, 11169 (1996).
[23] C. Wolverton, V. Ozolins, and M. Asta, Phys. Rev. B **69**, 144109 (2004).
[24] See EPAPS Document No. E-PRLTAO-101-007839 for the calculation details and further discussion. For more information on EPAPS, see http://www.aip.org/pubservs/epaps.html.
[25] D. B. Laks *et al.*, Phys. Rev. B **46**, 12587 (1992).
[26] Other shallow (Ag,Sb)Te ground states may exist, see Ref. [23], Section 2(c).
[27] J. P. McHugh *et al.*, J. Appl. Phys. **32**, 1785 (1961).
[28] A. Finel, Doctoral thesis, University of Paris Paris, 1987; Z. W. Lu *et al.*, Phys. Rev. B **44**, 512 (1991).
[29] C. Wolverton and A. Zunger, J. Electrochem. Soc. **145**, 2424 (1998).
[30] The deviations from the $x_{Sb} = x_{Ag}$ stoichiometry are discussed in Ref. [24] [Sec. 3(e)].
[31] D. L. Zhang and B. Cantor, Acta Metall. Mater. **39**, 1595 (1991).
[32] M. E. Thompson *et al.*, Acta Metall. Mater. **42**, 2107 (1994).
[33] M. M. Elembe, Proc. R. Soc. A **300**, 210 (1967); T. Seddon *et al.*, J. Mater. Sci. **11**, 1756 (1976).